P2-051

Mass spectrometry analysis of the impurity content in N_2 seeded discharges in JET-ILW

A. Drenik*[a], M. Oberkofler[b], D. Alegre[c], U. Kruezi[d], S. Brezinsek[e], M. Mozetič[a], I. Nunes[f], M. Wischmeier[b], C. Giroud[d], G. Maddison[d], C. Reux[g], and JET EFDA Contributors**

JET-EFDA, Culham Science Centre, Abingdon, OX14 3DB, UK

[a] *Jožef Stefan Institute, EURATOM Association Jamova 39, 1000 Ljubljana, Slovenia*
[b] *Max-Planck-Institut für Plasmaphysik, Boltzmannstraße 2, D-85748 Garching, Germany*
[c] *As. EURATOM-CIEMAT, Av. Complutense 40, 28040 Madrid, Spain,*
[d] *Culham Centre for Fusion Energy, Abingdon, Oxon, OX14 3DB, United Kingdom*
[e] *IEF - Plasmaphysik FZ Jülich, EURATOM Association, 52425 Jülich, Germany*
[f] *Associação EURATOM - IST, Instituto de Plasmas e Fusão Nuclear, 1049 - 001, Lisboa, Portugal*
[g] *CEA, IRFM, EURATOM Assoc, F-13108 St Paul Les Durance, France*

aleksander.drenik@ijs.si

Abstract Presented are the results of the first mass spectrometry study of impurities at JET with the ILW. Measurements are performed with the newly-installed RGA system that allows for data acquisition in all stages of machine operation. Impurities are predominantly found in the 16 – 20 AMU range, populated by water, methane and ammonia, and at 28 AMU (CO and N_2). The main contaminants in non-seeded discharges are deuterated methane and water, and nitrogen, which are present only in low amounts, and are likely produced by plasma-surface interaction. During N_2 seeded discharges, signals increase significantly at 28 AMU, but also in the 16 – 20 AMU range, indicating conversion of nitrogen to ammonia. In subsequent non-seeded discharges, impurity content is reduced by an order of magnitude, however it exhibits a 5 – 7 discharge-long legacy.

**See the Appendix of F. Romanelli et al., Proceedings of the 24th IAEA Fusion Energy Conference 2012, San Diego, USA

PACS: 52.25.Vy, 52.40.Hf, 52.55.Fa, 52.70.Nc

PSI-21 Keywords: Impurity, Impurity seeding, JET-ILW

Corresponding author:
Aleksander Drenik
Jožef Stefan Institute
Jamova 39
1000 Ljubljana
Slovenia

1. Introduction

Since the installation of the ITER-like wall (ILW), JET provides a unique test bed to study plasma operation in the ITER material mix: Be plasma-facing components (PFCs) in the main chamber and W components in the divertor [1]. W sputtering which determines the lifetime of the divertor components in the Be/W mix is dominated by intrinsic impurities such as Be, O and C, and extrinsic impurities like N_2 and Ar[2], though the C and Be content are orders of magnitude lower in quantity in comparison with the carbon wall[3]. As the JET-ILW does not include carbon-based PFCs, nitrogen is being seeded to replace carbon as the radiating species in the plasma edge and mitigate heat loads at the W target plates[4]. Argon is routinely used as gas for the disruption mitigation system in JET which injects massive amounts of Ar + D_2 mixture to reduce or prevent damage to PFCs caused by disruptions[5]. Therefore, a complex set of impurities can interact with the first wall and impact the plasma operation, and identification and quantification of these species and their temporal evolution as legacy gas is of interest.

In this paper, we present a residual gas analysis (RGA) study of the impurity content during N_2 seeded discharges at JET. Residual gas analysis relies on the use of mass spectrometers (MS), placed typically downstream of the plasma volume in pump ducts. As the transmission path from the plasma to the MS is long, charged particles, metastable species and neutral non-noble atoms do not reach the MS, and only the content of inert species (stable molecules and noble gases) can be analysed. However, unlike other diagnostic techniques that do not suffer from such limitations (such as VUV spectroscopy), the detection by MS provides information on the impurity content throughout all stages of the tokamak operation (discharge phase, outgassing after a disruption, time between discharges …). This contribution is the first report based on fast RGA measurements in JET-ILW with sufficient temporal resolution to monitor trends in the discharge phase.

2. Experimental

The impurity content of the tokamak vacuum vessel was analysed with a newly installed sub-divertor residual gas analysis system[6]. It is based on a Hiden Analytical HAL 201 RC mass spectrometer (MS), located in the sub-divertor. The spectrometer is placed inside a soft iron chamber for magnetic shielding, which enables accurate measurements in all stages of the discharge. The pressure in the sub-divertor reaches up to 10^{-3} mbar during

normal discharges, which exceeds the operational range of the MS. In order to allow RGA operation during discharges, the MS chamber is differentially pumped and connected to the main volume of the sub-divertor diagnostic system through a gas flow restrictor.

During discharges, the intensities at the following discrete mass to charge ratios were recorded: 2, 3, 4, 12, 13, 14, 15, 16, 17, 18, 19, 20, 21, 23, 28, 29, 30, 31, 32 and 40 AMU/e. The sampling time was 1.4 s which allowed for recording of several data points in the discharge flattop phase of about ten seconds. The set of masses was selected primarily for the purpose of N_2 seeded experiments. The 2 – 4 AMU range is expected to be populated by hydrogen species, the 15 – 20 AMU range is expected to be populated by ammonia, water and methane in H and D isotope configurations. Mass 28 AMU is expected to be populated primarily by N_2 (with a smaller signal at 14 AMU), but also by CO. Mass 32 AMU is attributed to O_2, mass 40 AMU to Ar (with a second peak at 20 AMU) and mass 44 to CO_2, however the higher end of the recorded range can also be populated by higher hydrocarbons. Since we expect no molecules or noble gases to contribute to the signal at 23 AMU, it is used for estimation of the noise level. The recording at 21, 29 and 30 AMU ($_{15}ND_3$, $_{15}N_{14}N$ and $_{15}N_2$ respectively) was set for the requirements of $_{15}N_2$ seeding experiments, however these data are not presented in this paper.

To analyze the discharge phase recordings, beside observing the time traces of RGA signals, we also observe time-integrated intensities at individual masses, with the background value subtracted (referred to as pulse integrals) [7]. The background value is defined as the mean value of the signal in a 40 second period before the start of the pulse. In all cases, the background signals were indistinguishable from noise, indicating that the background atmosphere of the instrument has no impact on the measurements. As the RGA system has not yet been calibrated, the intensities cannot be linked to absolute abundances of the detected species, and the cracking patterns used in the discussion are provided by the manufacturer of the MS, for a pure H system. The pulse integrals should therefore not be taken for absolute quantities of pumped gases, they nonetheless allow for observing trends of impurity content over a wide range of pulses.

The majority of the data used in this study is obtained from discharges between #JPN 85356 and 85462. This data set consists of uninterrupted RGA recordings of non-seeded sessions (#JPN 85356 – 85404), five consecutive nitrogen seeding sessions in which a total of 16.7 barl nitrogen was injected (#JPN 85405 – 85436), followed by another session without

nitrogen, however with deliberate argon injections (#JPN 85445 – 85457, 59.9 barl). This provides the opportunity to characterize the sub-divertor gas composition in non-seeded discharges, study the direct impact of seeding and its long-term legacy effects.

3. Results and discussion

The RGA recordings are studied in the following cases: Dry runs (gas injections without plasma operation) which provide information about impurities that are introduced during fueling, non-seeded discharges which provide information about the intrinsic impurity content and N_2 seeded discharges, which provide information about the RGA response during different seeding rates, the effect of N_2 seeding on the impurity content and the legacy of N_2 in subsequent non-seeded discharges.

3.1. Dry runs

In most cases, the impurity content in dry runs is below the level of detection, however when the volume of injected gas is comparable to that during discharges, some impurities can be detected in the 16 – 20 AMU range and at 28 AMU, as shown in Fig. 1a. The dominant impurity signal is at 20 AMU, followed by 18 and 19 AMU with significantly smaller intensities. The relative intensities make a relatively good match for the cracking pattern of deuterated water (D_2O and DO with 23 % the intensity). A faint signal at 28 AMU is also observed, but as its intensity barely rises above the noise level, the signal at 14 AMU, expected at roughly 10 % the intensity, could not be measured with sufficient accuracy to verify if the 28 AMU signal is due to N_2 or CO.

As seen in Fig 1b, the amount of impurities increases with injected volume of D_2. This could suggest that these impurities are introduced into the reactor vessel either through desorption in the gas lines, or desorption from the PFC surfaces. Additionally, deuterated water could also be formed in the RGA itself. In the present setup, however, it is not possible to discern between the possible contributions to these signals.

3.2. Non-seeded discharges

The time-trace of RGA signals at masses 18, 20 and 28 AMU during a non-seeded discharge is shown in Fig. 2b, along with the plasma heating power and the outer strike point position (Fig. 2a). The signals rise with the onset of the divertor phase (at 1.3 s). When the neutral beam injection (NBI) starts and the plasma transitions to H mode, intensities of RGA signals further increase. After the switch-back to L mode, intensities begin to decline until they fall back to the background around 25 seconds after the start of the pulse. The average values of pulse-integrals of non-seeded discharges are shown in Fig 3. It should be noted there that the values in the 1 – 4 AMU range, and at 20 and 40 AMU are obtained only from undisrupted discharges. As disruptions are followed by injections of the disruption mitigation gas (D_2 and Ar), the signals at 20 and 40 AMU are dominated by Ar (Ar^{++} and Ar^{+} respectively) which distorts the intrinsic impurity content statistics.

The signals at 4 AMU exceed all others by more than an order of magnitude, while the intensities at 23 AMU are at least an order of magnitude lower than the rest of the recordings, indicating that the recorded signals are clearly above the noise level. At the impurity related masses, pulse integrals of signals at 18 and 20 AMU are stronger than the rest of the 16 – 20 AMU range by an order of magnitude. Their relative intensities match the cracking pattern of deuterated methane (CD_4 and CD_3 with 80 % the intensity), which has also been reported in AUG[8]. The pulse integral at 28 AMU is also significant, accompanied by the pulse integral at 14 AMU with about 6 % the intensity, suggesting that a significant part of the signals at 28 AMU are due to N_2. Impurities are detected also at 32 AMU which could be due to O_2.

Fig 4 shows pulse integrals of 18, 20 (a and b), 28 and 32 (c and d) AMU plotted against the total volume of injected D_2 (a and c) and the time-integral of ohmic, RF and NBI power (b and d, labeled as input energy). The injected volume influences the pulse integrals only in the far-low end of the range (up to 2 barl). At higher volumes, the pulse integrals appear evenly scattered. Conversely, the pulse integrals continue to increase, albeit with a significant amount of scatter, all through the time-integrated power range. This suggests that the impurities in non-seeded discharges are produced by plasma-surface interaction, rather than injected with D_2 (as in the case of dry runs).

3.3. N_2 seeded discharges

The time-trace of the RGA signal at 28 AMU in a N_2 seeded discharge is shown in Fig 6 a) (JPN85410). Before the seeding starts, the signal rises due to "intrinsic" N_2. After the beginning of N_2 seeding (at 10 s), the intensity at further increases (with a 2 s response time), exceeding the intrinsic values by more than an order of magnitude. As it is being seeded, the majority of the signal can be safely interpreted as N_2.

The actual intensity of the RGA signal at 28 AMU depends on the amount of injected N_2, as shown in Fig. 5a, where the pulse integrals at 28 AMU exhibit a near linear dependence on the seeded volume. Moreover, N_2 seeding is reflected also in the rise in the 16 – 20 AMU range. The pulse integrals at all recorded masses are shown in Fig. 5c (JPN 86425), for the discharge with the largest amount of seeded N_2 (2.58 barl), where the strongest increase in the 16 – 20 AMU range is observed at 17 and 18 AMU. The observed increase at 30 AMU is most likely due to attachment of D atoms to the N_2 molecule in the RGA. The response to N_2 seeding at 17 and 18 AMU two masses is shown in Fig. 5b. Experiments both at AUG[8] and TEXTOR[9] have shown that N_2 seeding causes in-vessel ammonia formation, and that the produced ammonia exhibits a significantly higher H/D ratio that the in-vessel atmosphere, therefore the strongest increase would be expected in signals at masses lower than 20 AMU. Thus, the observed response at 17 and 18 AMU can be interpreted as indication that ammonia is being formed in N_2 seeded discharges.

The majority of N_2 seeded discharges take place in a single, almost uninterrupted series, during which a total 16.7 barl of N_2 is injected. In the following non-seeded discharges, the intensity of the RGA signal at 28 AMU is, while still an order of magnitude lower than during the seeding discharges, considerably higher than in the non-seeded discharges before the seeding session. The pulse integral at 28 AMU in the first non-seeded discharge after the seeding session is $1.2 \cdot 10^{-5}$ (a.u.), whereas the non-seeded average is $(6.5 \pm 3.4) \cdot 10^{-6}$ (a.u.). The time trace of RGA signals at 28 AMU in non-seeded discharges before (JPN 85402) and after (JPN 85438) the N_2 seeding session, a N_2 seeded discharge (JPN 85410) are shown in Fig. 6a. The signal at 28 AMU in JPN 85438 is considerably higher than at JPN 85402. Moreover, the behavior itself is different – the highest intensity is observed at the end of H mode. This suggests that N_2 that is retained after seeded discharges is released through different mechanisms than the "intrinsic" N_2.

Fig. 6b shows evolution of pulse integrated intensities at 28, 17 and 18 AMU versus pulse number, It takes between 5 and 7 discharges for the pulse integrals to come down to

average values. However, in subsequent discharges (deliberate disruptions and injections of Ar containing disruption mitigation gas), the decline of the pulse integrals continues below average values, suggesting that the observed behavior could in part be influenced by the machine operation and is perhaps not entirely attributable to N_2 retention exclusively.

4. Conclusions

The RGA measurements indicate low impurity content in JET with the ILW, with the main contaminants being deuterated water and methane, and nitrogen. The dry run recordings reveal that possible sources of impurities are desorption from the gas lines through which D_2 is passed and desorption from PFC surfaces, whereas in the non-seeded discharges, the more likely source of impurities is plasma-wall interaction.

In N_2 seeded discharges, intensities at 28 AMU clearly dominate the impurity content and exceed the intrinsic impurities content by an order of magnitude. Pulse integrated intensity at 28 AMU exhibits a close to linear dependence on the volume of seeded N_2. Moreover, N_2 seeding gives rise to increase of impurity content in the 16 – 20 AMU range, as is demonstrated by a close to linear dependence of pulse integrals at 17 and 18 AMU on the seeded N_2 volume as well.

While in subsequent non-seeded discharges, the intensities at 28 AMU, as well as in the 16 – 20 AMU range, are lower by an order of magnitude than in the seeded discharges, they are still considerably higher than the average non-seeded value and return to the average value in 5 – 7 discharges. The time traces at 28 AMU after N_2 seeded discharges exhibit different behaviour as in “standard” non-seeded discharges, indicating that release of retained N_2 takes place through different mechanisms than that of intrinsic N_2 (or other contributors to the signal at 28 AMU).

Following the reports of ammonia production at AUG[8] and TEXTOR[9], we find evidence of N_2 retention and ammonia production at JET. However, both the production of ammonia as well as retention and release of N_2 should be subject of further, dedicated experiments and analyses.

5. Acknowledgement

This work was supported by EURATOM and carried out within the framework of the European Fusion Development Agreement. The views and opinions expressed herein do not necessarily reflect those of the European Commission.

6. References

1. (a) Horton, L.; Contributors, E.-J., *Fusion Engineering and Design* 2013, *88* (6-8), 434-439; (b) Romanelli, F.; Contributors, J. E., *Nuclear Fusion* 2013, *53* (10).

2. Neu, R. L., et al., *IEEE Trans. Plasma Sci.* 2014, *42* (3), 552-562.

3. Brezinsek, S., et al., *J. Nucl. Mater.* 2013, *438*, S303-S308.

4. Giroud, C., et al., *Nuclear Fusion* 2013, *53* (11).

5. (a) Lehnen, M., et al., *Nuclear Fusion* 2011, *51* (12); (b) Lehnen, M., et al., *J. Nucl. Mater.* 2013, *438*, S102-S107.

6. Kruezi, U., et al., *Review of Scientific Instruments* 2012, *83* (10).

7. Oberkofler, M., et al., *J. Nucl. Mater.* 2013, (Supplement).

8. Neuwirth, D., et al., *Plasma Phys. Control. Fusion* 2012, *54* (8).

9. Garcia, A. C., et al., (this publication).

7. Figure captions

Fig. 1: a) Time-trace of RGA signals during a dry-run (JPN 85226), b) pulse-integrated intensities of RGA signals at 18, 20 and 28 AMU versus volume of injected D_2 during dry runs.

Fig. 2: Time trace of plasma heating power (a) and RGA signals at 18, 20 and 28 AMU (b) during a non-seeded pulse (JPN 85402)

Fig. 3: Average pulse-integrated intensities of RGA signals at impurity related masses in non-seeded discharges (values for 20 and 40 AMU obtained only from non-disrupted discharges).

Fig. 4: Pulse integrated intensities of RGA signals in non-seeded discharges, a) at 18 and 20* AMU versus total injected gas volume, b) at 18 and 20* versus time-integrated total plasma heating power, c) at 28 and 32 AMU versus total injected gas volume, d) at 28 and 32 AMU versus time-integrated total plasma heating power

* - values for 20 AMU are obtained only from non-disrupted discharges.

Fig. 5: a) Response of pulse-integrated intensities of RGA signals at 28 AMU to N_2 seeding, b) Response of pulse-integrated intensities at 17 and 18 AMU to N_2 seeding, c) Pulse integrals at the discharge with the largest seeded volume of N_2 (25.8 barl).

Fig. 6: a) Time-traces of RGA signals for a non-seeded discharge (JPN 85402), a N_2 seeded discharge (JPN 85410) and a non-seeded discharge following a N_2 seeding session (JPN 85438), b) Evolution of pulse-integrated intensities of RGA signals at 28, 17 and 18 AMU in non-seeded discharges following an N_2 seeding session.

8. Figures

Fig 1

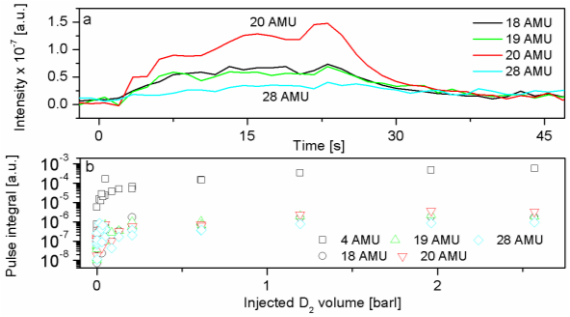

Fig. 2

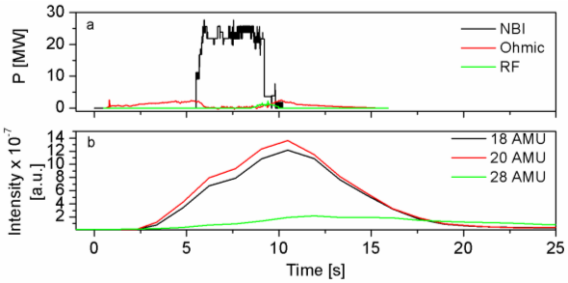
a
P [MW]
30
20
10
0
NBI
Ohmic
RF
b
Intensity x 10^-7 [a.u.]
14
12
10
8
6
4
2
18 AMU
20 AMU
28 AMU
0
5
10
15
20
25
Time [s]

Fig. 3

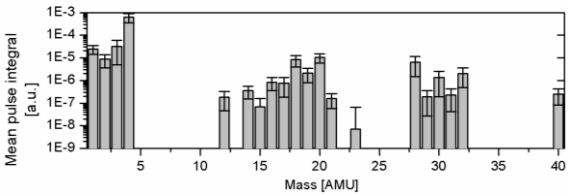
Mean pulse integral [a.u.]
1E-3
1E-4
1E-5
1E-6
1E-7
1E-8
1E-9
5
10
15
20
25
30
35
40
Mass [AMU]

Fig. 4

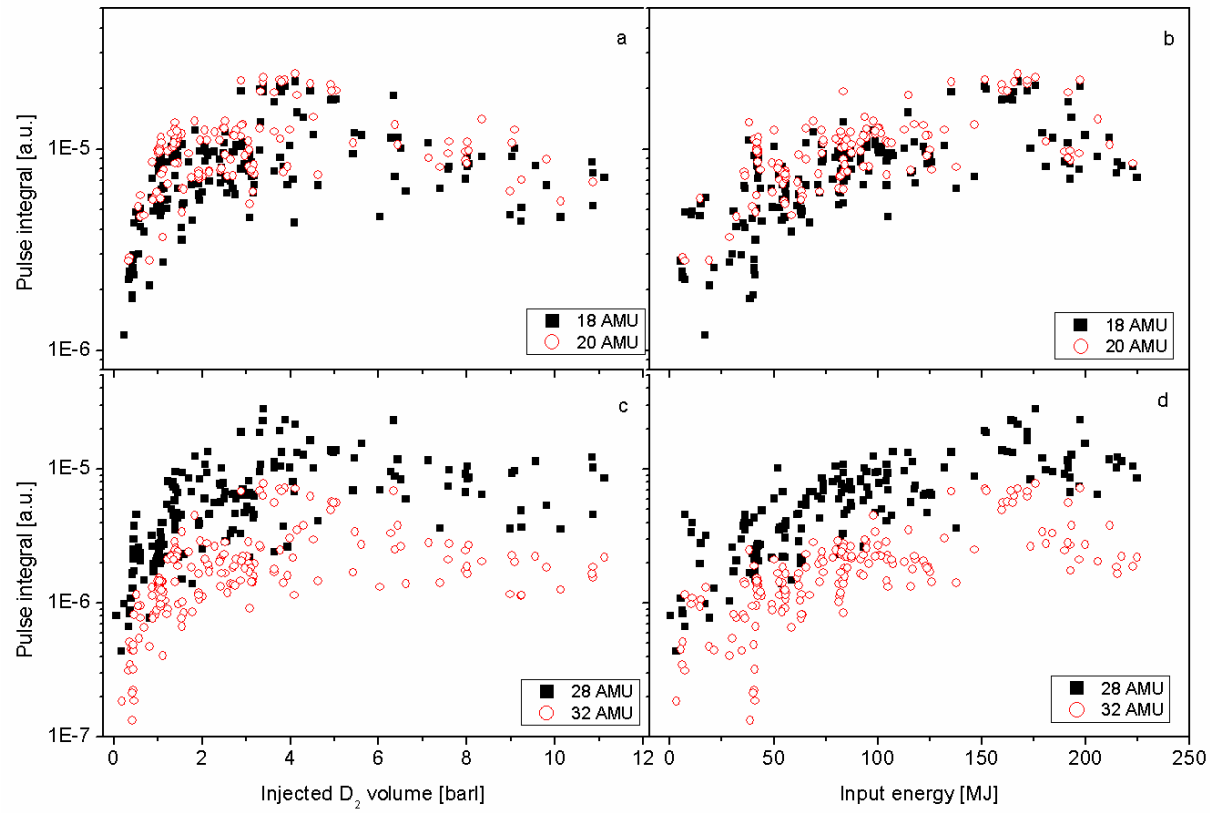
a
b
c
d
Pulse integral [a.u.]
1E-5
1E-6
1E-7
18 AMU
20 AMU
28 AMU
32 AMU
0
2
4
6
8
10
12
50
100
150
200
250
Injected D2 volume [barl]
Input energy [MJ]

Fig. 5

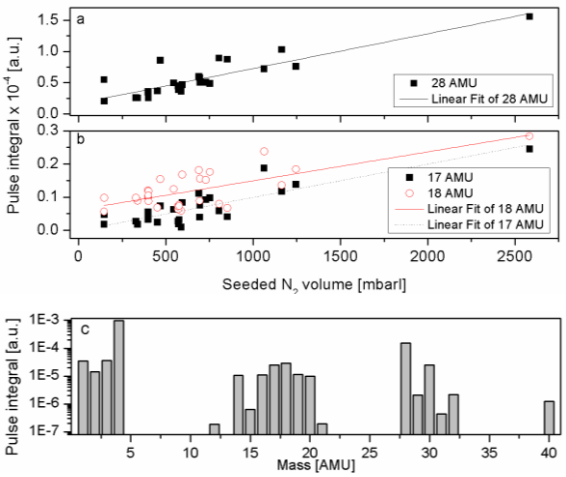
a
b
c
28 AMU
Linear Fit of 28 AMU
17 AMU
18 AMU
Linear Fit of 18 AMU
Linear Fit of 17 AMU
Pulse integral x 10⁻⁴ [a.u.]
Seeded N2 volume [mbarl]
Pulse integral [a.u.]
Mass [AMU]

Fig 6

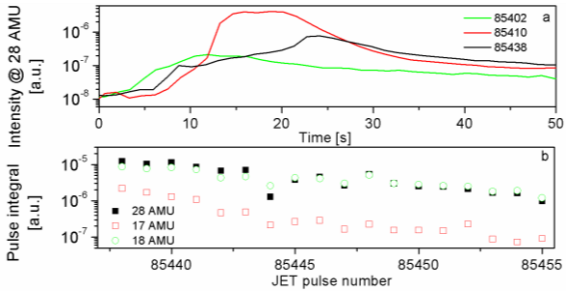
Intensity @ 28 AMU [a.u.]
85402
85410
85438
a
Time [s]
Pulse integral [a.u.]
28 AMU
17 AMU
18 AMU
b
JET pulse number